Beilstein Journal of Nanotechnology

Synthesis of indium oxi-sulfide films by atomic layer deposition: The essential role of plasma enhancement

Cathy Bugot*, Nathanaëlle Schneider, Daniel Lincot and Frédérique Donsanti*

Full Research Paper

Open Access

Address:
Institut de Recherche et Développement sur l'Energie Photovoltaïque (IRDEP), UMR 7174 – EDF – CNRS – Chimie Paristech, 6 quai Watier, 78401 Chatou, France

Email:
Cathy Bugot* - cathy-externe.bugot@edf.fr;
Frédérique Donsanti* - frederique.donsanti@edf.fr

* Corresponding author

Keywords:
atomic layer deposition; buffer layer; indium oxi-sulfide; plasma enhancement; thin film solar cells

Beilstein J. Nanotechnol. **2013,** *4,* 750–757.
doi:10.3762/bjnano.4.85

Received: 31 July 2013
Accepted: 24 October 2013
Published: 13 November 2013

This article is part of the Thematic Series "Energy conversion applications of atomic layer deposition".

Guest Editor: J. Bachmann

© 2013 Bugot et al; licensee Beilstein-Institut.
License and terms: see end of document.

Abstract

This paper describes the atomic layer deposition of $In_2(S,O)_3$ films by using $In(acac)_3$ (acac = acetylacetonate), H_2S and either H_2O or O_2 plasma as oxygen sources. First, the growth of pure In_2S_3 films was studied in order to better understand the influence of the oxygen pulses. X-Ray diffraction measurements, optical analysis and energy dispersive X-ray spectroscopy were performed to characterize the samples. When H_2O was used as the oxygen source, the films have structural and optical properties, and the atomic composition of pure In_2S_3. No pure In_2O_3 films could be grown by using H_2O or O_2 plasma. However, $In_2(S,O)_3$ films could be successfully grown by using O_2 plasma as oxygen source at a deposition temperature of T = 160 °C, because of an exchange reaction between S and O atoms. By adjusting the number of In_2O_3 growth cycles in relation to the number of In_2S_3 growth cycles, the optical band gap of the resulting thin films could be tuned.

Introduction

Chalcopyrite-type thin film solar cells that are based on a $Cu(In,Ga)Se_2$ (CIGS) absorber have reached high efficiencies, up to 20.3% [1] in 2011 and 20.4% [2] on flexible substrates in 2013. The best efficiencies were obtained by using cadmium sulfide (CdS) as buffer layer in solar cells with a glass/Mo/CIGS/CdS/i-ZnO/ZnO:Al stack. The buffer layer is an n-type semiconductor that forms the p–n junction with the p-type CIGS absorber, and also modifies the CIGS surface chemistry, which is usually too sensitive for a direct deposition of the window layers. However, because of the toxicity of cadmium and the low optical band gap of CdS (2.4 eV [3]) that limits the light conversion of CIGS in the UV range of the solar spectrum,

alternative materials have been developed. Most Cd-free buffer layers are based on zinc and indium-compounds, with current record efficiencies obtained by chemical bath deposition (CBD, 19.7% and 19.1% for Zn(S,O,OH) [4,5], 15.7% for In(S,O,OH) [6]) or atomic layer deposition (ALD, 18.5% for Zn(O,S) [7], 18.1% for (Zn,Mg)O [8], 16.4% for In_2S_3 [9], and 18.2% for (Zn,Sn)O [10]). Recently, our group has synthesized new mixed films of ZnS/In_2S_3 by using ALD and applied them as buffer layers in CIGS solar cells [11,12]. ALD is based on sequential self-saturated reactions that allows the conformal and uniform growth of thin films with a high control of their properties [13-15]. It is therefore a suitable technique for the deposition of buffer layers. Platzer-Björkman et al. have used ALD to improve the energy-band alignment between the CIGS and the front electrode by controlling the oxygen concentration in Zn(S,O) buffer layers [4,16]. Oxygen-doping of In_2S_3 films is known to increase their optical band gap value [6,17,18]. Indeed, by O-doping of In_2S_3 films deposited by thermal evaporation, Barreau et al. could increase the optical band gap value of In_2S_3 thin films from 2.1 to 2.9 eV [17]. In the same way, by using the spray pyrolysis technique, Maha et al. have inserted sulfur atoms in In_2O_3 thin films and obtained optical band gaps in the range from 3.85 to 3.96 eV [18]. Thus, based on our previous results and those studies, we became interested in adjusting the optical properties of In_2S_3 by incorporating oxygen atoms while using the advantages of ALD. Typical ALD processes for the deposition of In_2S_3 and In_2O_3 are referenced in Table 1. As ALD processes of In_2O_3 report relatively small growth rates, we will consider the case of plasma enhancement. Indeed, plasma-enhanced ALD (PEALD), in which various reactive species are generated, has been the key for the development of fast thin-film deposition processes at low temperature. It is widely used to enhance the thin-film deposition of materials such as Al_2O_3, ZnO, Ta_2O_5, TiN, TaN and SiN_x [19].

In this study, ALD and PEALD have been used to synthesize $In_2(S,O)_3$ thin films and carry out optical band-gap engineering. The structural, optical and growth properties of the films will be studied and the role of the plasma will be discussed.

Results

Study of $In(acac)_3$, H_2S and H_2O system

First, a controlled growth of pure In_2S_3 films was established and the film properties were measured in order to clearly identify the influence of oxygen pulse later in the study. For that, In_2S_3 growth was achieved in the temperature range between 140 and 240 °C. An In_2S_3 growth cycle consists of the following steps: $In(acac)_3$ exposure/N_2 purge/H_2S exposure/N_2 purge = 0.1/5/0.1/5 s, the relative long purge time being chosen to ensure a good homogeneity. Figure 1a shows the growth rate of In_2S_3 thin films at various temperatures. It globally increases with the temperature. An ALD window can be speculatively observed between 160 °C and 200 °C with a mean growth rate of 0.84 Å/cycle. The variation of the In_2S_3 growth rate with different $In(acac)_3$ pulse lengths at a process temperature of 160 °C is illustrated in Figure 1b. This variation only slightly influences the growth rate and a saturation by lengthening the precursor pulse is not observed. The data suggest that the results displayed on Figure 1a may not have been obtained under completely self-limiting conditions. Structural and optical properties of the films were also investigated. In_2S_3 thin films have an amorphous structure for deposition temperatures below 180 °C and a β-tetragonal crystal structure at higher temperatures. Their indirect optical band gap varies from 2.0 eV to 2.2 eV.

Then, we attempted to synthesize $In_2(S,O)_3$ film by inserting an In_2O_3 growth cycle. For this H_2O was pulsed, instead of H_2S in the growth of pure In_2S_3, which led to the supercycles $n\cdot\{In_2S_3\} + \{In_2O_3\}$ with n = 1,2,3,5,9,14,19, which corres-

Table 1: Typical ALD processes for the deposition of In_2O_3 and In_2S_3.

reactant A	reactant B	temperature (°C)	growth rate (Å/cycle)	reference
		indium oxide		
$InCl_3$	H_2O	500	0.27	[20]
InCp	$O_3/O_2/H_2O$	250	1.3/0.16/0.068	[21]
InCp	H_2O & O_2	100–250	1.0–1.6	[22]
TmIn	H_2O	217	0.39	[23]
$In(acac)_3$	H_2O/O_3	165–225	0.2/0.12	[24]
		indium sulfide		
$InCl_3$	H_2S	300	1.4	[25]
$In(acac)_3$	H_2S	160, 180, 160, 150	0.6, 0.7, 0.44, 0.3	[9,26-28]

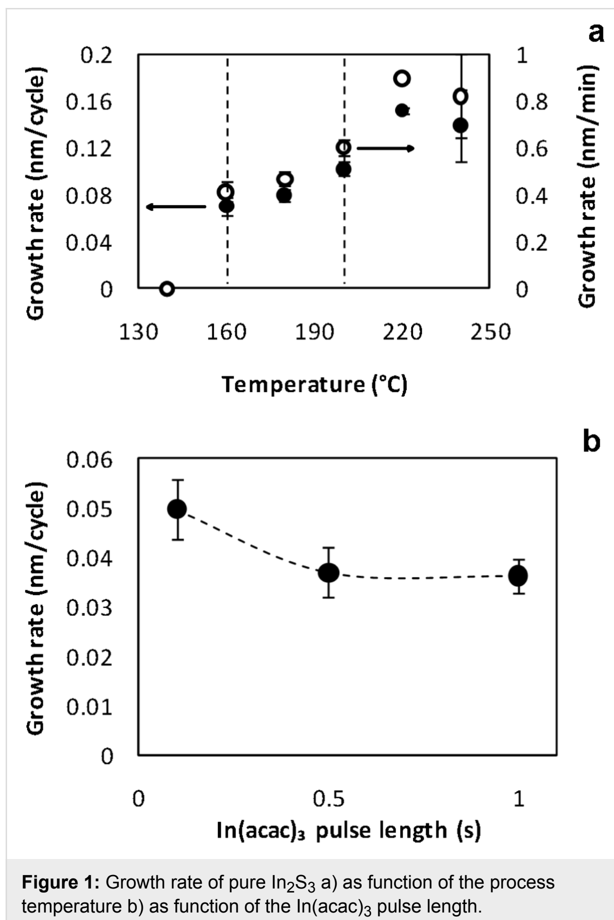

Figure 1: Growth rate of pure In_2S_3 a) as function of the process temperature b) as function of the $In(acac)_3$ pulse length.

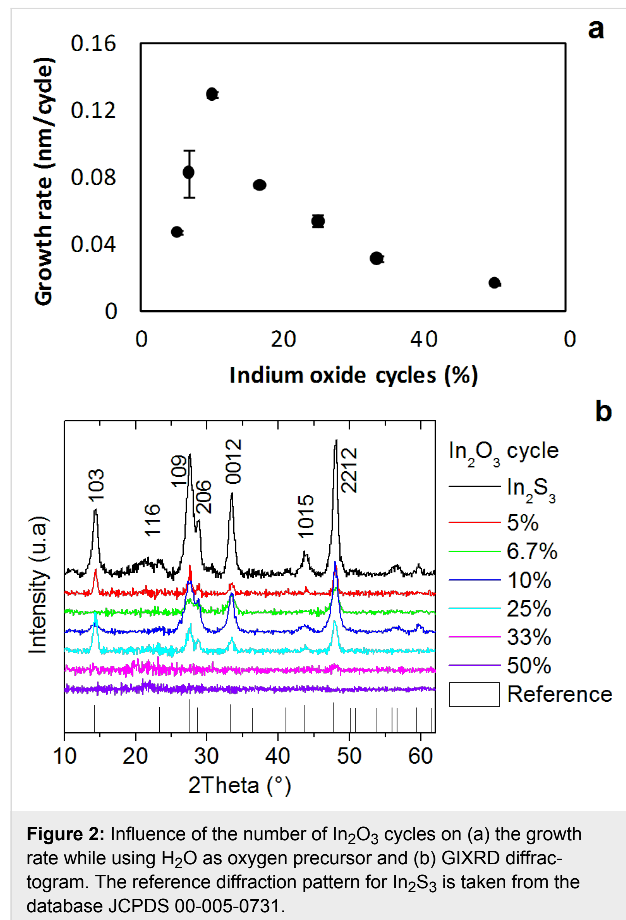

Figure 2: Influence of the number of In_2O_3 cycles on (a) the growth rate while using H_2O as oxygen precursor and (b) GIXRD diffractogram. The reference diffraction pattern for In_2S_3 is taken from the database JCPDS 00-005-0731.

pond to ratios of {50%, 33%, 25%, 10%, 6.7%, 5%} of In_2O_3 cycles at a deposition temperature of 200 °C. All samples were deposited performing a total of 2000 growth cycles, i.e., 100 supercycles for n = 19, 133 supercycles for n = 14, etc. Energy dispersive X-ray spectroscopy analysis was performed on the samples and gave atomic ratios of 0.4 for In/(In+S) and 0.6 for S/(In+S), which correspond to typical In_2S_3 atomic ratios. The oxygen contents are similar to those of pure In_2S_3 films, which is assigned to the oxygen contamination of the substrate. Those results were confirmed by GI-XRD measurements. They were performed to investigate the influence of the H_2O pulse on the microstructure of the films (Figure 2b). Not all samples were crystalline and the crystalline ones can be attributed to β-In_2S_3 with a random orientation by comparing the diffraction patterns with the reference data and with the literature [27]. Indeed, we should observe a peak shift due to increasing oxygen doping when changing the In_2O_3/In_2S_3 ratio. However, the peaks remain at the same diffraction angles. Comparing the FWHM of the (109) peak, the maximum FWHM measured was 1.2° for the 10%-In_2O_3 sample, which corresponds to the thickest film. In general it can be said that the thinner the films, the lower the FWHM. From these observations, it seems that we obtained In_2S_3 films only.

Thin films optical absorption were determined from transmittance (T) and reflectance (R) measurements by using the following formula [29]

$$\alpha = -\frac{1}{t} \cdot \ln\left(\frac{(1-T)}{R}\right),$$

where α is the absorption coefficient and t is the film thickness. Figure 3 shows absorption spectra of the thin films. They are presented in the form of $(\alpha)^{0.5} = f(E)$, which is linear for indirect band gap materials and allows for the determination of the optical transition. The optical band gaps correspond to an indirect transition in the range from 1.9 to 2.2 eV, which is roughly similar to that of pure In_2S_3 film optical properties. No correlation could be found between either the ratio of In_2O_3 cycles or the film thickness and the optical measurements. These results are in accordance with the observations of the structural analysis. Consequently, this method is not suitable to synthesize $In_2(S,O)_3$ thin films. In parallel, we attempted to synthesize pure In_2O_3 films from $In(acac)_3$ and H_2O at temperatures of 160 and 200 °C. This remained unsuccessful, because no films could be grown under these conditions.

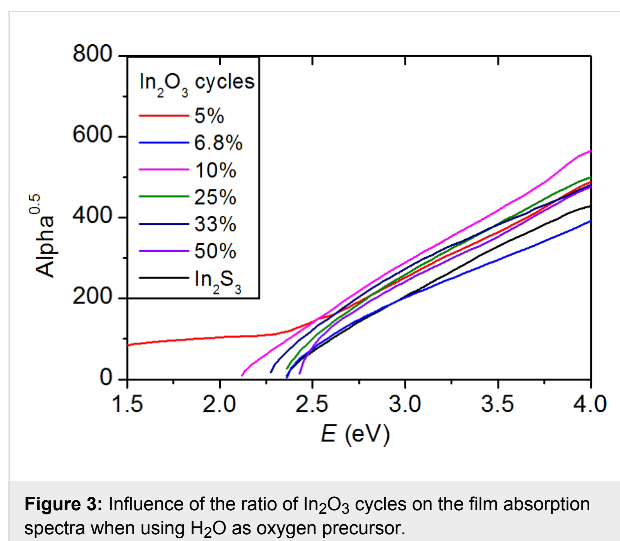

Figure 3: Influence of the ratio of In_2O_3 cycles on the film absorption spectra when using H_2O as oxygen precursor.

Study of the $In(acac)_3$, H_2S and O_2 plasma system

As O_2 plasma is known to have a different reactivity, it was evaluated as potential oxygen source for the deposition of $In_2(S,O)_3$. Thin film syntheses were performed by incorporating In_2O_3 growth cycles that use O_2 plasma pulses in the growth of In_2S_3: $In(acac)_3$ exposure/N_2 purge/O_2 + plasma exposure/N_2 purge = 0.1/5/7/3 s in the following supercycles $n\cdot\{In_2S_3\} + 2\cdot\{In_2O_3\}$ with n = 15,20,25,30,35,40 which correspond to ratios of {11.8%, 9.1%, 7.4%, 6.25%, 5.4%, 4.8%} of In_2O_3 cycles at a deposition temperature of 160 °C. A total of 2000 cycles was achieved for all samples as described in the previous section. The dependence of the growth rate on the number of In_2O_3 cycles is shown in Figure 4a. When increasing the ratio from 4.8% to 9.1%, the growth rate increases up to 1.4 Å/cycle and then decreases again. The variation of the film thickness with the number of ALD cycles for a ratio of 10% of In_2O_3 cycles is illustrated in Figure 4b. A linear growth is observed up to 1500 ALD cycles. GIXRD measurements revealed an amorphous structure in all the samples.

Transmittance and reflectance measurements were carried out on the $In_2(S,O)_3$ samples. Figure 5 shows the transmittance of $In_2(S,O)_3$ films as a function of the percentage of In_2O_3 cycles. A shift of the onset absorption can be observed, which suggests an evolution in the properties of the films. The indirect optical transitions were identified for all samples from their respective absorption spectra (Figure 6a). The values are plotted as a function of the ratio of In_2O_3 cycles in Figure 6b. The maximum value corresponds to the theoretical optical gap of In_2O_3 [30]. The optical band gaps vary from 2.2 ± 0.1 eV for pure In_2S_3 to 3.3 ± 0.1 eV for $In_2(S,O)_3$ and increase with the number of In_2O_3 cycles during the deposition process of In_2S_3.

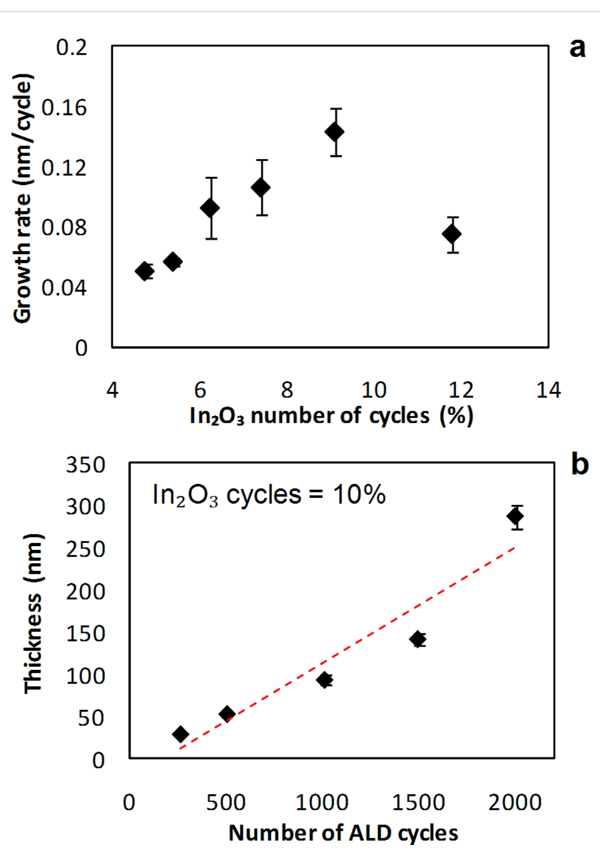

Figure 4: Influence of a) the number of In_2O_3 cycles on the growth rate b) the number of process cycles on the film thickness when using O_2 plasma as oxygen precursor. The dotted line is a guide to the eyes.

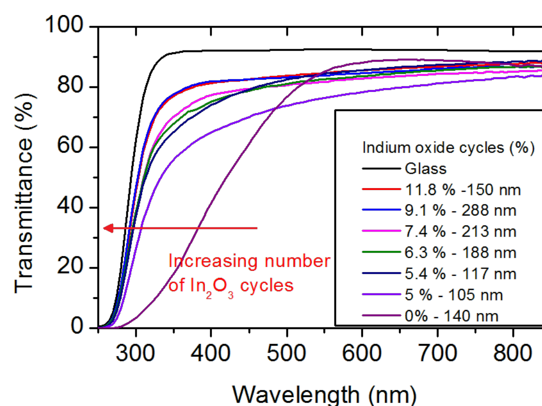

Figure 5: Influence of the number of In_2O_3 cycle on the film transmittance when using O_2 plasma as oxygen precursor.

The atomic ratios of oxygen, sulfur and indium determined by using EDX are presented in Table 2 and correlated to the optical band gap values. The dependence of the atomic ratio of oxygen and the optical band gap on the number of In_2O_3 cycles is not clear. In general, high oxygen concentrations of more than 66 atom % were measured in the films.

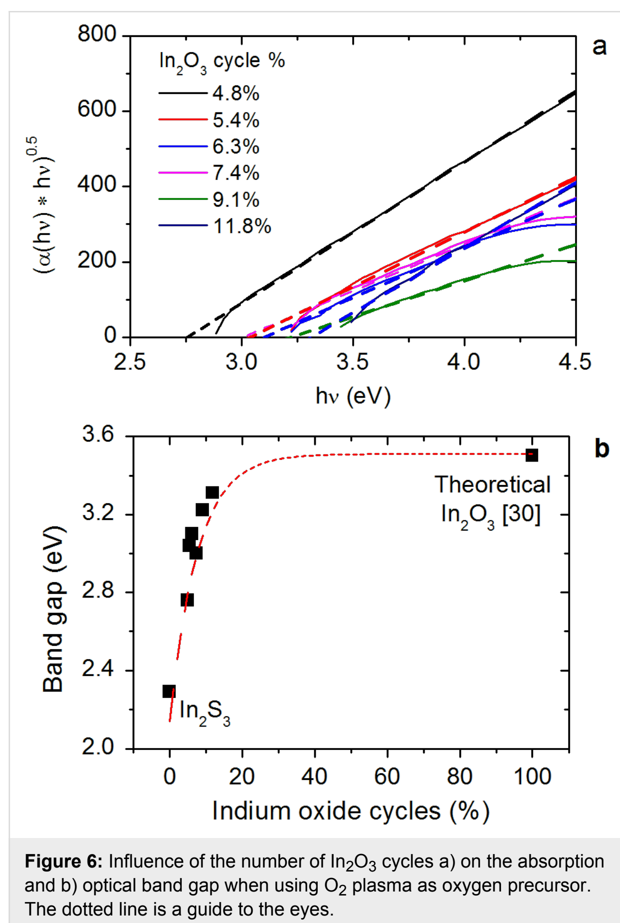

Figure 6: Influence of the number of In_2O_3 cycles a) on the absorption and b) optical band gap when using O_2 plasma as oxygen precursor. The dotted line is a guide to the eyes.

We also tried to synthesize $In_2(S,O)_3$ by using a single O_2 plasma pulse instead of In_2O_3 pulse cycles. The following cycle program was used: 20·{In_2S_3} + 2·{O_2+plasma exposure}/N_2 purge with the same process parameters. This corresponds to 9.1% of indium cycles, which can be compared to the previous deposition with a pulse of $In(acac)_3$ before the O_2 plasma exposure. Table 3 shows the properties of these two samples, along with those of pure In_2S_3. Even without the $In(acac)_3$ pulse, O and S atomic ratios indicate that the synthesized film corresponds to a $In_2(S,O)_3$ film and no significant differences were observed between the samples.

The growth of $In_2(S,O)_3$ growth could be achieved when using O_2 plasma as oxygen precursor. The maximum growth rate was 1.4 Å/cycle, which is higher than the growth rates of In_2S_3 shown in Figure 1 and those reported in the literature for this deposition temperature [9,26-28]. Optical measurements revealed an onset absorption moving to higher energies when increasing the number of In_2O_3 cycles. At the same time, the optical band gap increased from 2.2 eV to 3.3 eV for In_2O_3 cycle ratios in the range from 0 to 11.8%. EDX analysis showed that those films have a high oxygen content. Finally, all attempts to synthesize pure In_2O_3 films from $In(acac)_3$ and O_2 plasma remained unsuccessful .

Discussion

It has been observed that inserting an In_2O_3 cycle during the deposition of In_2S_3 when using H_2O as oxygen precursor has no influence on the oxygen content and on the film properties. It only affects the growth rate as the thickness varies. Attempts to synthesize pure In_2O_3 thin films were also unsuccessful, which suggests a low reactivity of H_2O towards $In(acac)_3$. Several authors reported the difficulty to synthesize In_2O_3 by ALD using β-diketonates ($In(acac)_3$, In(hfac = hexafluoropenta-

Table 2: EDX measurements data from $In_2(S,O)_3$ thin films when using O_2 plasma.

In_2O_3 (%)	optical band gap (eV)	(O+S)/(In+S+O) (atom %)	In/(In+S+O) (atom %)	S/(In+S+O) (atom %)	O/(In+S+O) (atom %)
4.80	2.76	83	17	15	68
5.41	3.04	85	15	10	75
6.25	3.10	85	15	11	74
7.41	3.00	80	20	14	66
9.09	3.22	79	21	10	69
11.76	3.31	83	17	9	74

Table 3: Comparison between $In_2(S,O)_3$ films, synthesized with and without $In(acac)_3$ during the oxidation pulse, and In_2S_3.

program	E_g (eV)	growth rate (Å/cycle)	In/(In+S+O) (atom %)	S/(S+O) (atom %)	O/(S+O) (atom %)
20·{In_2S_3} + 2·{In_2O_3}	3.2 ± 0.1	1.4 ± 0.2	21	13	87
20·{In_2S_3} + 2·O_2 plasma	3.3 ± 0.1	1.2 ± 0.2	17	15	85
In_2S_3	2.2 ± 0.2	0.7 ± 0.08	35	70	30

dionate)$_3$, In(thd = 2,2,6,6-tetramethyl-3,5-heptanedioneate)) and water [20,21,25]. In most cases, they assigned the low growth rates or the absence of grown films to the low reactivity of water toward β-diketonates.

As no pure In_2O_3 films could be grown in our case, the synthesis of mixed films by a simple addition of two layers, i.e., In_2O_3 + In_2S_3, is not possible. However, the deposition of ternary materials can also occur via exchange reactions. For instance, when synthesizing zinc indium sulfide (ZIS) thin films, substitution mechanisms between diethylzinc (DEZ) and In_2S_3 could be demonstrated [11]. Similar mechanisms also occur when inserting H_2O in pure ZnS during the growth of Zn(S,O) by using ALD [4,16]. Such processes do not seem to occur in our case, because the $In_2(S,O)_3$ deposition method that uses H_2O remained unsuccessful. A possible thermodynamic explanation for the unfavorable deposition of $In_2(S,O)_3$ using H_2O as oxygen precursor is that the following exchange reaction is endothermic and thus unlikely to occur [31].

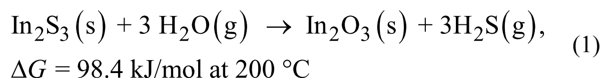

$$In_2S_3(s) + 3\,H_2O(g) \rightarrow In_2O_3(s) + 3H_2S(g),\quad \Delta G = 98.4 \text{ kJ/mol at } 200\ °C \qquad (1)$$

Due to the high reactivity of radicals, PEALD generally allows the achievement of many chemical reactions that cannot occur with thermal ALD [13,19]. Here $In_2(S,O)_3$ films could be grown while using O_2 plasma as oxygen source. But the growth of pure In_2O_3 films remained unsuccessful. This suggests that the oxygen contained in $In_2(S,O)_3$ films is not generated from single layers of In_2O_3 but rather by exchange reactions as described in the previous section. Indeed, the O_2 plasma can directly react with the film surface and induce an exchange reaction with surface sulfur atoms. Figure 7 presents a scheme of the assumed substitution mechanism at the surface.

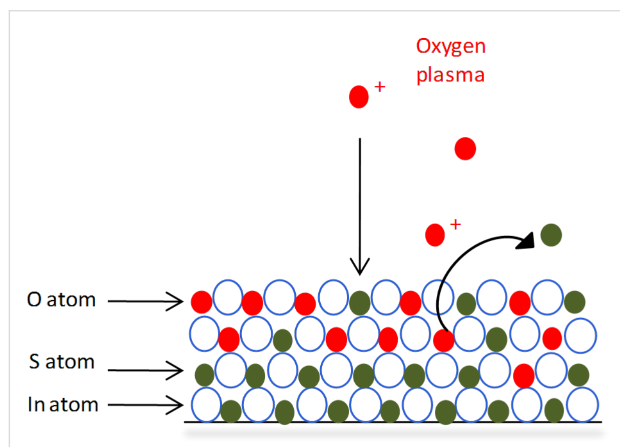

Figure 7: Surface mechanisms during the O_2 plasma pulse.

The following exchange reactions can explain the substitution of S atoms by reactive oxygen species generated in the plasma. Indeed, their free standard enthalpies all have negative values:

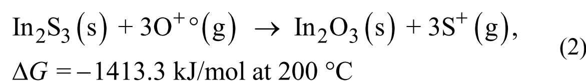

$$In_2S_3(s) + 3O^{+\circ}(g) \rightarrow In_2O_3(s) + 3S^{+}(g),\quad \Delta G = -1413.3 \text{ kJ/mol at } 200\ °C \qquad (2)$$

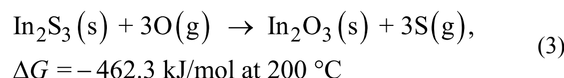

$$In_2S_3(s) + 3O(g) \rightarrow In_2O_3(s) + 3S(g),\quad \Delta G = -462.3 \text{ kJ/mol at } 200\ °C \qquad (3)$$

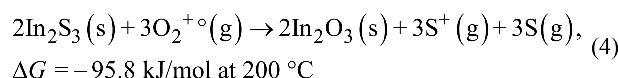

$$2In_2S_3(s) + 3O_2^{+\circ}(g) \rightarrow 2In_2O_3(s) + 3S^{+}(g) + 3S(g),\quad \Delta G = -95.8 \text{ kJ/mol at } 200\ °C \qquad (4)$$

Thus, when comparing these reactions with the reaction between In_2S_3 and H_2O, it seems that the doping is only favorable when using O_2 plasma as oxygen precursor, because these reactions are all exothermic. This thermochemical analysis and the observation that $In_2(O,S)_3$ films obtained from the two different ALD pulse programs $20\cdot\{In_2S_3\} + 2\cdot\{In_2O_3\}$ and $20\cdot\{In_2S_3\} + 2\cdot O_2$ plasma have similar properties, show the critical role of activated oxygen during the deposition of $In_2(S,O)_3$.

Commonly existing species in oxygen plasmas are atomic oxygen that is created from molecular oxygen dissociation, excited oxygen species at different electronic levels, ionized oxygen or recombined species like O_3 [32,33]. Consequently, exchange reactions between adsorbed oxygen and oxygen species from the gas phase or recombination reactions have to be considered. Marinov et al. studied the interactions between a radiofrequency O_2 plasma and oxide surfaces like TiO_2, SiO_2 and Pyrex [32]. They demonstrated that these materials surfaces are continuously re-structured under O_2 plasma exposure because of the exchange reactions that occur between O atoms in the films and oxygen species of the gas phase. They also reported that reaction products undergo oxidation at the surface and assumed that two surface mechanisms could occur; $O + O \rightarrow O_2$ and $O + O_2 \rightarrow O_3$. Such mechanisms might also occur in our case considering the exchange reactions described in Figure 7 during the first O_2 plasma pulse. Indeed, no match was found between the ratios of In_2O_3 cycles during the deposition of $In_2(S,O)_3$ films and the oxygen content of the films determined by EDX. When the number of In_2O_3 cycles varied from 4.8% to 11.8%, in the same time the oxygen content of the films varied from 68 atom % to 75 atom %. Oxidation mechanisms during deposition process can explain these high differences between the expected values and those measured.

Comparing $In_2(S,O)_3$ films synthesized with and without an $In(acac)_3$ pulse before the O_2 plasma pulse, no significant differences in the band gap values or the atomic ratios of the samples were observed. This confirms that the formation of an In_2O_3 single layer is not required to synthesize $In_2(S,O)_3$ films. These results are in fair agreement with the fact that the growth of pure In_2O_3 remained unsuccessful. Thus, we can assume that only activated oxygen is involved during the deposition of $In_2(S,O)_3$, and In_2S_3 can be considered as an intermediate state for the formation of $In_2(S,O)_3$.

On-going studies focus on a better understanding on the nature of the oxygen species generated by the plasma, their role in oxidizing mechanisms and the reason of the relatively low indium content. One of them could be an excessive adsorption of oxygen in the film and the formation of sulfates. Further studies, in particular by using X-ray photoelectron spectroscopy, are in progress to assess the presence or not of such groups. Experiments will also be performed to study the influence of other oxygen sources such as O_2 alone and O_3.

Conclusion

In this study we reported the atomic layer deposition of $In_2(S,O)_3$ films by using $In(acac)_3$ (acac = acetylacetonate), H_2S, and either H_2O or O_2 plasma as oxygen sources. $In_2(S,O)_3$ films could only be obtained with O_2 plasma as oxygen source, and all attempts to synthesize In_2O_3 remained unsuccessful. Thus, synthesis of $In_2(S,O)_3$ films is likely to occur through an exchange reaction instead of simple mixing of In_2S_3 and In_2O_3 layers. A thermochemical analysis can explain such observations. Indeed, this reaction is endothermic for H_2O and exothermic for O_2 plasma.

With this new synthesis method, the optical band gap of the thin films could be tuned from 2.2 eV to 3.3 eV by increasing the number of O_2 plasma pulses. The high oxygen contents measured in the films (>66 atom %) in comparison to the initial number of In_2O_3 pulses might be explained by the fact that oxidation mechanisms occurred on the film surfaces during the O_2 plasma pulses. Due to the reactivity of the plasma, the film surfaces cannot be considered as a static system but should rather be seen as continually re-structured surfaces. In our future studies, those films will be applied as buffer layer in $Cu(In,Ga)Se_2$ solar cells to investigate their suitability as Cd-free buffer layer for thin film solar cells.

Experimental

In_2S_3 and $In_2(S,O)_3$ thin films were deposited on borosilicate glass and Si(100) substrates in a SUNALE R-200 ALD reactor (Picosun Oy.) with a modified 15 cm × 15 cm square reaction chamber. All samples were deposited performing a total of 2000 growth cycles. The source material for indium was indium acetylacetonate ($In(CH_3COCHCOCH_3)_3$), $In(acac)_3$, (98%, Strem Chemicals). Hydrogen sulfide, H_2S (99.5%, Messer) was used as the sulfur source. Deionized Millipore vapor water and O_2, (99.9995%, Messer) were used as oxygen source. O_2 was introduced in a remote RF plasma generator with Argon (99.9997%, Messer) as carrier gas, and the plasma power was kept at 2600 W. All sources were kept at room temperature while $In(acac)_3$ was heated to 200 °C. The carrying and purge gas was nitrogen with a purity of 99.9999% (Messer). The pressure in the reaction chamber was kept in the range from 1 to 4 mbar.

The thickness of the films was measured using a VEECO DEKTAK 6M profilometer on glass substrates. Thicknesses were determined after creating steps in the films, by masking film parts with chemically resistant tape and dipping the film in nitric acid (45% in water) at room temperature for 60 s. The uncertainty given for the thickness is the standard deviation of six measurements taking into account the uncertainty of the profilometer, the sharpness of steps, the film roughness, and the film inhomogeneity. Transmittance and reflectance spectra were obtained by using a PerkinElmer lambda 900 Spectrophotometer with a PELA-1000 integrating sphere. All optical measurements were performed on borosilicate glass substrates. X-Ray diffraction (XRD) studies were performed under grazing incidence X-ray diffraction conditions with a PANalytical Empyrean diffractometer while using Cu Kα radiation. X-Ray reflectometry analyses were also performed to confirm thickness measurements. Thin film compositions were obtained by using a Magellan 400L scanning electron microscope provided by FEI. It is equipped with an energy dispersive X-ray spectroscopy detector INCASynergy 350. All EDX measurements were carried out on Si(100) substrates and the values reported are atomic percentages (atom %).

Acknowledgements

This work is supported by Ministry of Higher Education and Research via Pierre and Marie Curie University (UPMC, ED390) and EDF. Energy Dispersive X-Ray Specroscopy measurements were performed by S.Borenztajn (CNRS) and Laboratoire de Photonique et Nanostructures (CNRS).

References

1. Jackson, P.; Hariskos, D.; Lotter, E.; Paetel, S.; Wuerz, R.; Menner, R.; Wischmann, W.; Powalla, M. *Prog. Photovoltaics* **2011,** *19,* 894–897. doi:10.1002/pip.1078
2. Empa – CIGS. http://www.empa.ch/plugin/template/empa/*/79143 (accessed July 31, 2013).
3. Çetinörgü, E.; Gümüş, C.; Esen, R. *Thin Solid Films* **2006,** *515,* 1688–1693. doi:10.1016/j.tsf.2006.06.004

4. Nakamura, M.; Kouji, Y.; Chiba, Y.; Hakuma, H.; Kobayashi, T.; Nakada, T. Achievement of 19.7% efficiency with a small-sized Cu(InGa)(SeS)2 solar cells prepared by sulfurization after selenizaion process with Zn-based buffer. 38th IEEE Photovoltaic Specialists Conference, June 3–8, 2012; Austin, TX.
5. Hariskos, D.; Menner, R.; Jackson, P.; Paetel, S.; Witte, W.; Wischmann, W.; Powalla, M.; Bürkert, L.; Kolb, T.; Oertel, M.; Dimmler, B.; Fuchs, B. *Prog. Photovoltaics* **2012,** *20,* 534–542. doi:10.1002/pip.1244
6. Hariskos, D.; Ruckh, M.; Rühle, U.; Walter, T.; Schock, H. W.; Hedström, J.; Stolt, L. *Sol. Energy Mater. Sol. Cells* **1996,** *41–42,* 345–353. doi:10.1016/0927-0248(96)80009-2
7. Zimmermann, U.; Ruth, M.; Edoff, M. In *21st European Photovoltaic Solar Energy Conference: Proceedings of the international conference held in Dresden,* Dresden, Germany, Sept 4–8, 2006; pp 1831–1834.
8. Platzer-Björkman, C.; Hultqvist, A.; Pettersson, J.; Törndahl, T. *Proc. SPIE* **2010,** *7603,* 76030F. doi:10.1117/12.846017
9. Naghavi, N.; Spiering, S.; Powalla, M.; Cavana, B.; Lincot, D. *Prog. Photovoltaics* **2003,** *11,* 437–443. doi:10.1002/pip.508
10. Lindahl, J.; Zimmermann, U.; Szaniawski, P.; Torndahl, T.; Hultqvist, A.; Salome, P.; Platzer-Bjorkman, C.; Edoff, M. *IEEE J. Photovoltaics* **2013,** *3,* 1100–1105. doi:10.1109/JPHOTOV.2013.2256232
11. Genevée, P.; Donsanti, F.; Renou, G.; Lincot, D. *J. Phys. Chem. C* **2011,** *115,* 17197–17205. doi:10.1021/jp203604j
12. Genevée, P.; Donsanti, F.; Renou, G.; Lincot, D. Atomic Layer Deposition of ZnInxSy Buffer Layers For Copper Indium Gallium Diselenide Thin Film Solar Cells. In *26th European Photovoltaic Solar Energy Conference and Exhibition: EU PVSEC Proceedings,* Hamburg, Germany, Sept 5–8, 2011; pp 2428–2431. doi:10.4229/26thEUPVSEC2011-3CO.4.4
13. Miikkulainen, V.; Leskela, M.; Ritala, M.; Puurunen, R. L. *J. Appl. Phys.* **2013,** *113,* 021301. doi:10.1063/1.4757907
14. van Delft, J. A.; Garcia-Alonso, D.; Kessels, W. M. M. *Semicond. Sci. Technol.* **2012,** *27,* 074002. doi:10.1088/0268-1242/27/7/074002
15. Bakke, J. R.; Pickrahn, K. L.; Brennan, T. P.; Bent, S. F. *Nanoscale* **2011,** *3,* 3482–3508. doi:10.1039/c1nr10349k
16. Platzer-Björkman, C.; Törndahl, T.; Abou-Ras, D.; Malmström, J.; Kessler, J.; Stolt, L. *J. Appl. Phys.* **2006,** *100,* 044506. doi:10.1063/1.2222067
17. Barreau, N.; Marsillac, S.; Albertini, D.; Bernede, J. C. *Thin Solid Films* **2002,** *403–404,* 331–334. doi:10.1016/S0040-6090(01)01512-7
18. Maha, M. H. Z.; Bagheri-Mohagheghi, M.-M.; Azimi-Juybari, H.; Shokooh-Saremi, M. *Phys. Scr.* **2012,** *86,* 055701. doi:10.1088/0031-8949/86/05/055701
19. Kim, H. *Thin Solid Films* **2011,** *519,* 6639–6644. doi:10.1016/j.tsf.2011.01.404
20. Asikainen, T.; Ritala, M.; Leskelä, M. *J. Electrochem. Soc.* **1994,** *141,* 3210–3213. doi:10.1149/1.2059303
21. Elam, J. W.; Martinson, A. B. F.; Pellin, M. J.; Hupp, J. T. *Chem. Mater.* **2006,** *18,* 3571–3578. doi:10.1021/cm060754y
22. Elam, J. W.; Libera, J. A.; Hryn, J. N. *ECS Trans.* **2011,** *41,* 147–155. doi:10.1149/1.3633663
23. Lee, D.-J.; Kwon, J.-Y.; Lee, J. I.; Kim, K.-B. *J. Phys. Chem. C* **2011,** *115,* 15384–15389. doi:10.1021/jp2024389
24. Nilsen, O.; Balasundaraprabhu, R.; Monakhov, E. V.; Muthukumarasamy, N.; Fjellvåg, H.; Svensson, B. G. *Thin Solid Films* **2009,** *517,* 6320–6322. doi:10.1016/j.tsf.2009.02.059
25. Asikainen, T.; Ritala, M.; Leskelä, M. *Appl. Surf. Sci.* **1994,** *82–83,* 122–125. doi:10.1016/0169-4332(94)90206-2
26. Yousfi, E. B.; Weinberger, B.; Donsanti, F.; Cowache, P.; Lincot, D. *Thin Solid Films* **2001,** *387,* 29–32. doi:10.1016/S0040-6090(00)01838-1
27. Sterner, J.; Malmström, J.; Stolt, L. *Prog. Photovoltaics* **2005,** *13,* 179–193. doi:10.1002/pip.595
28. Sarkar, S. K.; Kim, J. Y.; Goldstein, D. N.; Neale, N. R.; Zhu, K.; Elliott, C. M.; Frank, A. J.; George, S. M. *J. Phys. Chem. C* **2010,** *114,* 8032–8039. doi:10.1021/jp9086943
29. Hishikawa, Y.; Nakamura, N.; Tsuda, S.; Nakano, S.; Kishi, Y.; Kuwano, Y. *Jpn. J. Appl. Phys.* **1991,** *30,* 1008–1014. doi:10.1143/JJAP.30.1008
30. Liu, D.; Lei, W. W.; Zou, B.; Yu, S. D.; Hao, J.; Wang, K.; Liu, B. B.; Cui, Q. L.; Zou, G. T. *J. Appl. Phys.* **2008,** *104,* 083506. doi:10.1063/1.2999369
31. *HSC Chemistry;* Chemistry Software Ltd, 2013.
32. Marinov, D. Adsorption réactive des molécules et radicaux sur des surfaces sous exposition plasma. Ph.D. Thesis, Ecole Polytechnique X, Palaiseau, France, 2012.
33. Lopaev, D. V.; Malykhin, E. M.; Zyryanov, S. M. *J. Phys. D: Appl. Phys.* **2011,** *44,* 015202. doi:10.1088/0022-3727/44/1/015202

License and Terms

This is an Open Access article under the terms of the Creative Commons Attribution License (http://creativecommons.org/licenses/by/2.0), which permits unrestricted use, distribution, and reproduction in any medium, provided the original work is properly cited.

The license is subject to the *Beilstein Journal of Nanotechnology* terms and conditions: (http://www.beilstein-journals.org/bjnano)

The definitive version of this article is the electronic one which can be found at:
doi:10.3762/bjnano.4.85